

CFD Investigation of a MONJU 169-pin wire-wrapped fuel assembly experiment

Seongchul Park^a, Jae-Ho Jeong^{a*}

^aMechanical Engineering, Gachon University, Seongnam-si, Gyeonggi-do, 13120

*Corresponding author: jaeho.jeong@gachon.ac.kr

***Keywords** : Sodium Fast Reactor, Wire-wrapped fuel assembly, CFD, single channel analyzer

1. Introduction

The use of liquid metal coolant is a critical element in many fast reactor technologies, emphasizing the need for the development of appropriate modeling techniques to enhance our understanding of liquid metal coolant. Liquid Metal Fast Reactors (LMFR) are expected to play a significant role in the future of nuclear energy due to their exceptional heat transfer properties, wide availability, high power density, and improved safety. Within the core of a nuclear reactor, heat generated by nuclear fuel initiates nuclear chain reactions, serving as the source of nuclear fission energy. The reactor core typically consists of multiple fuel assemblies, each comprising numerous fuel rods. Wire spacers, wound around the fuel rods, are commonly used to maintain separation between the rods and enhance heat transfer efficiency. This wire spacer design is standard in sodium-cooled fast reactor (SFR) core configurations and promotes effective coolant mixing. In this scenario, sodium coolant enters through inlet nozzles, absorbs heat from the fuel pins, rises along the wire spacers, circulates around the fuel pins, and exits through outlets. While the presence of wire spacers complicates the flow behavior of liquid metal coolants, a comprehensive understanding of heat transfer phenomena within the nuclear fuel assembly is essential for the overall reactor design and safety assessment.

The evaluation of heat transfer within wire-wrapped fuel bundles plays a crucial role in assessing reactor design and safety. It directly impacts temperature distribution, thereby determining the maximum temperatures of both the coolant and the cladding. In this context, simulations of heat transfer within the reactor core are of paramount importance for safety assessment and reactor design. However, it is essential to recognize that applying experimental correlations of heat transfer behavior between liquid metal and the fuel bundle often introduces significant uncertainties. Conducting experiments in this field is challenging primarily due to the high costs and substantial experimental uncertainties associated with technologies such as Particle Image Velocimetry (PIV), used to detect velocity fields and precisely measure temperature distributions in liquid metal. To address these challenges, experts in the nuclear industry are increasingly emphasizing numerical analysis methods, especially simulation techniques such as CFD, which are becoming heavily reliant on numerical analysis approaches and computational technology [1].

Nevertheless, it remains crucial to underscore that methodologies developed based on CFD should undergo rigorous validation against experimental data. Unfortunately, due to limited availability and access to relevant experimental databases, achieving comprehensive validation of modeling approaches related to heat transfer poses difficulties. Moreover, in many cases, a lack of consideration for CFD validation, and the absence of crucial information and solutions in experimental data, make it virtually impossible to recover omitted details. In this study, our objective is to acquire data from specific experimental reports, refine it for CFD-based research, and perform a comprehensive and detailed analysis. By appropriately validating this data, our research highlights the successful application of CFD methodologies developed and validated primarily using limited benchmark data for investigating heat transfer phenomena.

A comprehensive analysis of thermal phenomena within the fuel assembly involves evaluating several critical factors. These factors include assessing sodium pressure drops and temperature distributions under normal operating conditions, investigating flow phenomena under low-flow scenarios, including natural circulation, blockage effects, and boiling effects. The temperature distribution within the fuel assembly is influenced by various contributing factors, including axial and radial power distribution within the assembly, mass flow distribution in each sub-channel, wire spacer configuration, and the effects of turbulence and mixing. Researchers Kabir and Hayafune analyzed cooling water temperature distribution using low-flow supercritical sodium boiling experimental data and simulated Loss-of-Flow (LOF) events in the PLANDL facility [2]. They also evaluated the predictive capabilities of the SuperSystem Code (SSC) and Subassembly Boiling Evolution Analysis (SABENA) code using data related to radial temperature distribution and boiling tests [2]. The PLANDTL facility, detailed in the following section, was designed to replicate the conditions experienced during a Loss-of-Piping-Integrity (LOPI) event in the MONJU reactor, with the aim of collecting thermal-hydraulic experimental data for the fuel assembly. Concurrently, code analysis using SSC and SABENA, validated through these experiments, was conducted to investigate the performance during a temporary LOPI event. Subsequent experiments employed the validated SSC and SABENA codes to examine LOPI transients within the MONJU reactor. The simulation of LOPI

events predicted that sodium boiling would occur within certain parts of the fuel assembly, even when operating conditions were close to rated power levels.

In this study, we conducted CFD simulations using the STAR-CCM+ simulation software, employing the Reynolds-Averaged Navier-Stokes (RANS) method. The primary objective of this study was to evaluate the capability of software in predicting heat transfer phenomena within the MONJU reactor's 169-pin wire-wrapped fuel bundle. Our main goal was to assess the fluid dynamics and heat transfer characteristics of the MONJU reactor under specific operating conditions using CFD. This assessment included a comparative analysis to ensure the reliability and consistency of the results obtained from the CFD simulations. The ultimate aim of this investigation was to provide valuable insights and recommendations for selecting robust modeling tools for the design and operation of Liquid Metal Reactors (LMR).

2. Test section description

2.1 Test explanation

Experimental studies on the 169-pin wire-wrapped fuel assembly were conducted within the Sodium Boiling and Fuel Failure Propagation test loop, known as SIENA, at the Oarai Engineering Center of PNC. The primary aim of these experiments was to validate the results of the experiment using multidimensional hydrothermal code AQUA [3].

2.2 Test equipment

Fig. 1 depicts the test section of the 169-pin fuel assembly [4]. The design specifications of the 169-pin fuel assembly are detailed in Table 1. This fuel bundle consists of 169 pins arranged in a hexagonal pattern with a pitch-to-diameter ratio of 1.21. The pins have a diameter of 6.5 mm and are centered within the hexagonal tubes with a flat-to-flat distance of 104.6 mm. Each 169-pin is surrounded by a wire spacer with a diameter of 1.26 mm and encapsulated by a 306 mm-long cladding. The fuel rod length within the 169-pin assembly is 930 mm. Figure 1 illustrates the electrically heated segments of the 169-pin bundle located 350 mm downstream from the entrance of the fuel assembly.

2.3 Test conditions

Test conditions are set in the range of 25 ~ 167 W/cm line output, 50 ~ 1200 L/min flow rate, and 200 ~ 500°C inlet temperature. A range of dimensionless numbers in the test conditions performed is $Re = 2,500 \sim 55,000$ and $Pe = 13 \sim 230$. In addition, the test cases and their conditions to be used in the validation of the analysis conditions are listed in Table 2.

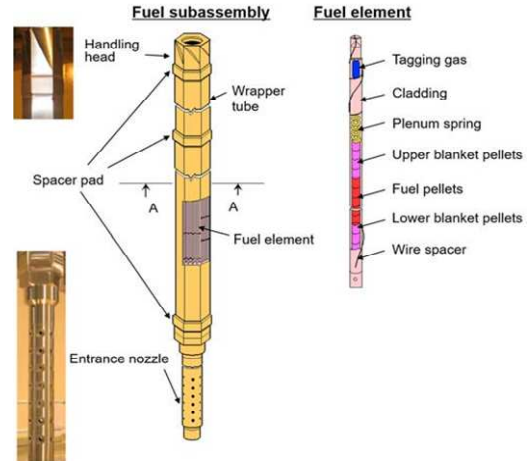


Fig. 1. 169-pin fuel assembly with sodium.

Table 1: Geometric parameters of fuel assembly.

Geometric parameters	Values
Number of pins	169
Pin diameter	6.5 [mm]
Pin pitch	7.86 [mm]
Spacer wire diameter	1.26 [mm]
Spacer wire lead [mm]	306 [mm]
P/D	1.21
H/D	47.07
Wrapper tube inner flat to flat distance	104.6 [mm]
Wrapper tube thickness	3 [mm]
Inlet unheated length	350 [mm]
Heated length	930 [mm]
Outlet unheated length	1459 [mm]
Axial power profile	Uniform

Table 2: Test conditions of 169-pin fuel assembly

Case	Heating value [kW]	Inlet volumetric flow rate [L/min]	Inlet velocity [m/s]	Inlet temperature [°C]
MCH7-1789ABC-03A	27.45	198.64	0.905	392.28
MCH3-17C-01A	6.863	59.83	0.273	392.54

3. Numerical analysis method

3.1 Test section for numerical analysis

Fig. 2 shows the test section with numerical analysis conducted on the duct wall at the heated locations within the hexagonal duct, along with an overview of the heater pin arrangement in the MONJU 169-pin fuel assembly. Similar to Fig. 2, this CFD investigation was conducted using the full-scale experimental facility of the MONJU 169-pin fuel assembly. In particular, the pressure distribution on the duct wall within the heated test section exhibits a periodic pattern in a spiral shape, matching the wire spacer lead pitch length. In this study,

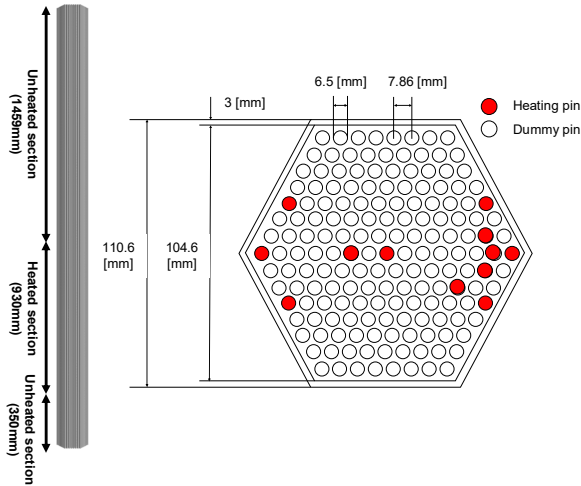


Fig. 2. Schematic of the 169-pin wire-wrapped fuel assembly.

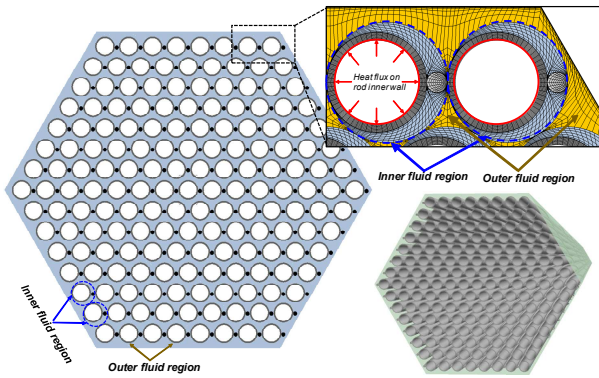


Fig. 3. Computational grid systems of 169-pin wire-wrapped fuel bundle.

3D flow and vortex phenomena were examined using RANS simulations with the Shear-Stress Transport (SST) turbulence model. High-resolution schemes were employed in these simulations to enhance accuracy. The convergence of the simulations was monitored and evaluated by observing the periodic temperature fluctuations at the outlet region of the 169-pin fuel assembly.

3.2 Computational grids and boundary conditions

Fig. 3 illustrates the computational grid configuration for the fuel assembly. An innovative grid generation method was adopted using custom Fortran-based code [5]. To account for heat conduction-based heat transfer in both the rod and wire, additional grids for the rod and wire were created, replicating the experimental setup and introducing two interfaces. This approach allows maintaining the actual wire shape without distortion, enabling a more accurate prediction of the contact area between the wire and rod.

Previous simulations using this approach demonstrated the capability to accurately predict pressure drops and analyze the flow within the fuel assembly [6]. In this study, the geometric details of the fuel bundle, including the rod and wire diameters, were

Table 3: Computational grids system.

Grid region	Cells	Nodes	Elements
Subchannels	37,229,200	41,113,652	37,229,200
Cladding	16,528,200	18,292,560	16,528,200
Wire	2,754,700	3,353,636	2,754,700
Total	56,512,100	62,759,848	56,512,100

Table 4: Boundary condition of CFD analysis.

Boundary domain	Condition	Value
Inlet	Constant velocity	Various
Outlet	Relative pressure	0 [Pa]
Rod outer	No slip (Smooth wall)	-
Wire outer		
Duct wall	No slip (Adiabatic)	-
Heat source (clad inner surface)	Constant heat flux	Various
Turbulence model	SST k- ω (Steady)	-

rigorously simulated. Table 3 provides detailed information about the computational grid system, divided into two domains: the fluid section and the structural section, facilitated by the internal mesh generation code. The total number of cells in the computational grid within the system is approximately 6.39×10^7 cells. Table 4 outlines the computational boundary conditions for the CFD analysis of the test assembly. The outer rod and outer wire are set to have a smooth roughness for non-slip conditions, and the duct wall is set to have a no-slip and adiabatic condition. The heat source is maintained constant over time, as indicated in Table 4.

3.3 Turbulence model

There are three main numerical analysis techniques: Direct Numerical Simulation (DNS), Large Eddy Simulation (LES), and RANS simulation. To accurately analyze the behavior of eddies in a turbulent field that includes various scales of eddies, it is important to ensure that the grid size is smaller than the minimum spatial scale of the eddy structure, and the time step is shorter than the minimum time scale of eddy fluctuations. DNS directly solves governing equations based on spatial scales without relying on turbulence models [7]. As a result, DNS is primarily suitable for flows with low Reynolds numbers or relatively simple geometries but requires extensive computational resources due to its resource-intensive nature. In contrast, LES directly calculates eddies larger than the grid scale using spatially-averaged Navier-Stokes equations and employs subgrid-scale (SGS) models to describe eddies smaller than the grid scale [8]. However, both DNS and LES require significant computational

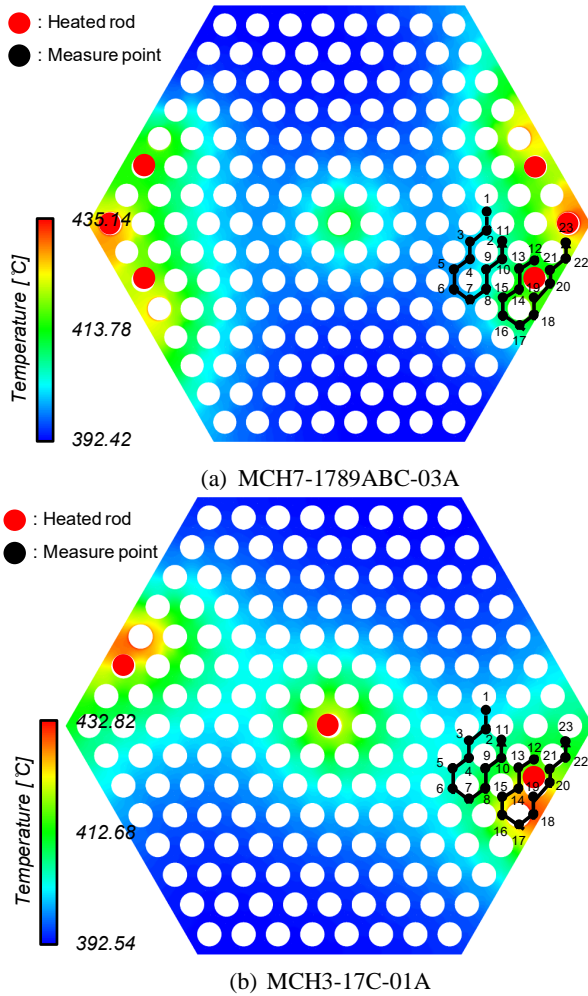


Fig. 4. Temperature field at top of heated section.

resources, making them impractical for many engineering applications.

In contrast, LES models the entire range of turbulent effects using time-averaged Navier-Stokes equations. LES provides coarser resolutions compared to DNS or LES, but due to its practicality, it finds widespread application in engineering scenarios. The advantage of LES lies in its ability to enhance computational efficiency by not requiring high-resolution computational grids, making it well-suited for a wide range of industrial and engineering applications.

The turbulence model used aims to calculate the Reynolds stress tensor by accounting for turbulence fluctuations in fluid momentum. Popular turbulence models such as $k-\epsilon$, $k-\omega$, and SST have become industry standards and are widely employed in various engineering applications. However, it's important to note that the $k-\epsilon$ model has limitations when dealing with high-pressure gradients, and the $k-\omega$ model can be overly sensitive to the characteristics of inlet freestream turbulence [9,10]. The SST model addresses these issues by smoothly transitioning between the $k-\epsilon$ model in the freestream region and the $k-\omega$ model in the viscous sub-layer [11]. To accurately capture the transition from laminar to turbulent flow using the SST

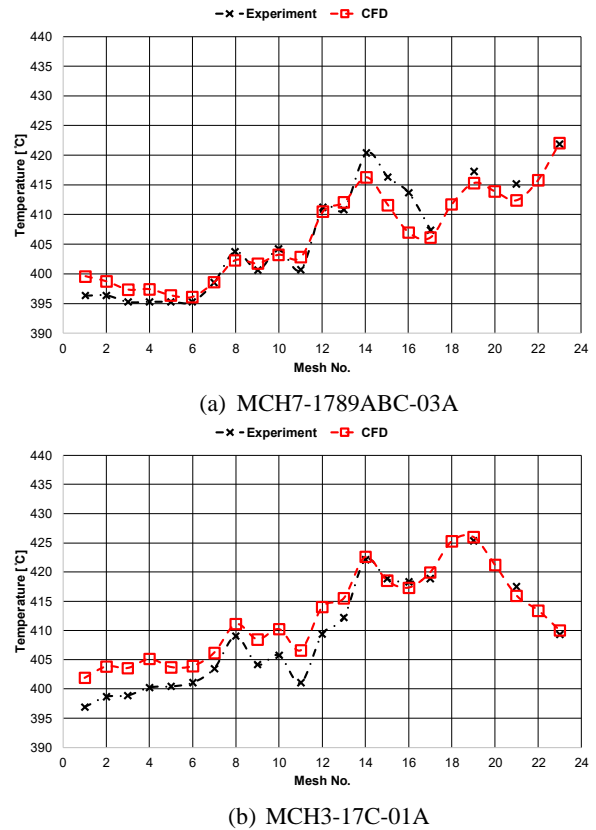


Fig. 5. Comparison of temperature distributions at the top end of heated section.

turbulence model, a minimal grid scale of $5.0 \times 10^{-7} \text{m}$ was used on the fuel rod walls to maintain a friction velocity (y^+) close to 1.

4. Results

As shown in Fig. 4, to compare the results in each radial direction, the mesh number was assigned according to the position of the subchannel, and each numbered mesh was analyzed. Fig. 5 shows the temperature distribution of the numerical study obtained using STAR-CCM+ and the experimental data. Since the PNC report only provides results for the top of the heated section, the comparison with this CFD analysis was made at the top of the heated section.

5. Conclusions

In this study, RANS based CFD methodology validation was performed on MONJU 169-pin fuel assembly experiment data for the high-precision CFD analysis technique using STAR-CCM+ code. CFD results are well matched with MONJU 169 pin fuel assembly experiment data. In the future, we plan to validate the reliability and consistency by comparing CFD resulting using the MARS-LMR code.

Acknowledgement

This work was supported by Korea Institute of Energy Technology Evaluation and Planning (KETEP) grant funded by the Korea government (MOTIE)(RS-2023-00243201, Global Talent Development project for Advanced SMR Core Computational Analysis Technology Development).

REFERENCES

- [1] Nuclear Energy Agency, Computational fluid dynamics for nuclear reactor safety applications-6 (CFD4NRS-6), Committee ON the Safety of Nuclear Installations, NEA/CSNI/R, 2017.
- [2] M.E. Kabir and H. Hayafune, Study of thermohydraulic behavior within the fuel bundle under a loss of flow condition, Power Reactor and Nuclear Fuel Development Corporation, PNC TN9410 92-018, 1992.
- [3] Muramatsu Juharu, Maekawa Isamu, Matsumoto Masahiko, "Single-phase multi-dimensional thermal-hydraulic analysis code : AQUA; Input manual, PNC TN9520 87-011, 1987.
- [4] P. Tamagno, W.F.G. van Rooijen, Uncertainty analysis of the prototype FBR Monju with the JENDL-4.0 nuclear data set, *Annals of Nuclear Energy*, Volume 51, 2013, 257-273.
- [5] Yamamoto, K., "An Elliptic-hyperbolic Grid Generation Method and Application to Compressor Flows.", Special Publication of National Aerospace laboratory, SP 19, pp. 193-198, 1992.
- [6] Jae-Ho Jeong, Min-Seop Song, Kwi-Lim Lee, "RANS based CFD methodology for a real scale 217-pin wire-wrapped fuel assembly of KAERI PGSFR", *Nuclear Engineering and Design*, vol. 313, pp.470-485, 2017.
- [7] Kawamura, H., Ohsaka, K., Abe, H., Yamamoto, K., 1998. DNS of turbulent heat transfer in channel flow with low to medium-high prandtl number fluid. *Int. J. Heat Fluid Flow* 19, 482-491
- [8] Smagorinsky, J., 1963. General circulation experiments with the primitive equations. I. The basic experiment. *Mon. Weather Rev.* 91, 99-165.
- [9] Bardina, J.E., Huang, R.G., Coakley, T.J., 1997. *Turbulence Modeling Validation, Testing, and Development*. NASA TM-110446.
- [10] Wilcox, D.C., 1998. Re-assessment of the scale-determining equation for advanced turbulence models. *AIAA J.* 26 (11), 1299-1310.
- [11] Menter, F.R., 1994. Two-equation eddy-viscosity turbulence models for engineering applications. *AIAA J.* 32 (8), 1598-1605.